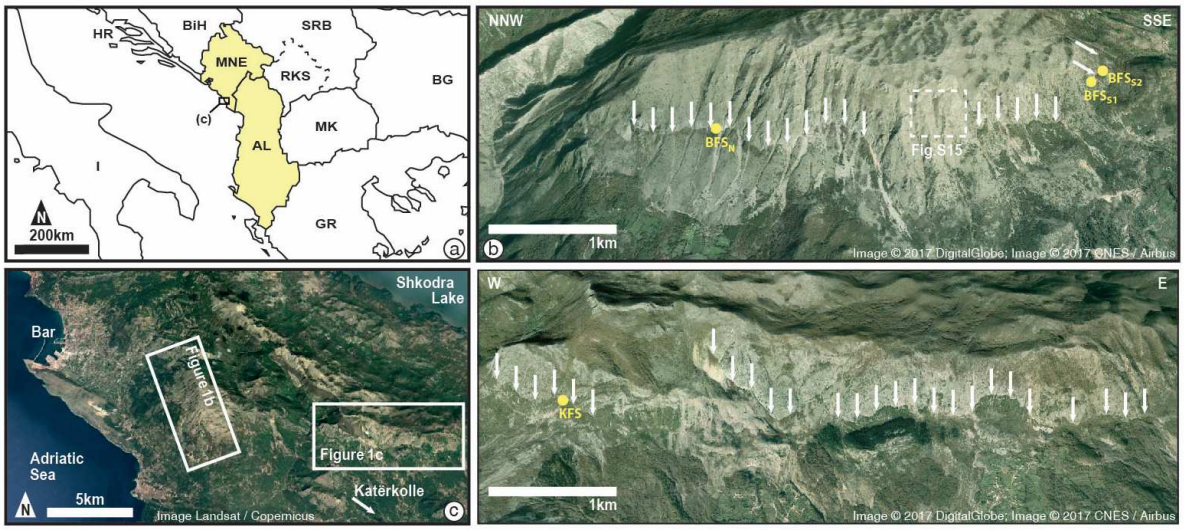

Figure S1: Google Earth©-based views of BFS and KFS. (a) Geographical position of the study area in the context of the Southern Adriatic region. (b) Google Earth©-based oblique view of BFS. The course of the fault scarp is traced by white arrows. Sampling sites are indicated by yellow dots. (c) Regional overview from satellite imagery. (d) Google Earth©-based oblique view of KFS. The course of the fault scarp is traced by white arrows. Sampling sites are indicated by yellow dots.

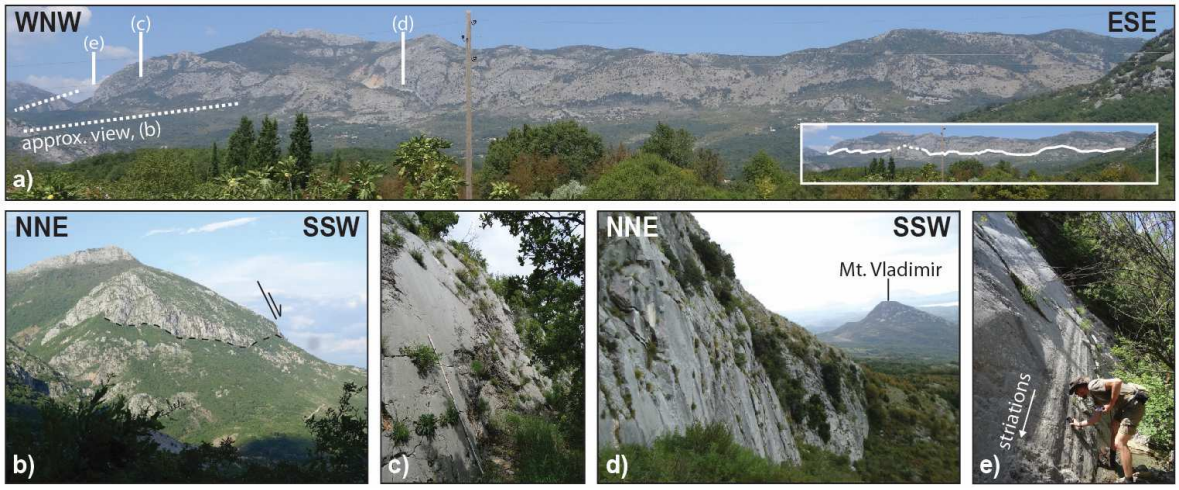

Figure S2: Photographs of KFS: (a) Panoramic view, small inset shows the fault trace, (b) topographic step in W part of KFS shows the trace of the fault scarp and degraded scarp in profile view, (c) profiling site KFS, 2-m ruler for scale. For localization of KFS see Fig. 3, (d) close-up view along the fault plane/free face; Mt. Vladimir (487 m a.s.l.) in the background, (e) fault plane of transfer fault at NW-most tip of KFS with striations indicating strong strike-slip component.

Table S3: Localization of fault scarp sections and sampling sites. Coordinates are given in degrees, minutes, seconds (WGS84). Lithological information is based on Geological survey of Yugoslavia (1971; see also Fig. 4). Section lengths refer to the observed surface ruptures (that might be exceeded by the total fault length).

Section	End 1	End 2	Lithology	Length [km]
BFS_N	42°4'29.98"N 19°9'38.21"E	42°3'16.38"N 19°10'10.63"E	Upper Triassic limestones and dolomites	ca. 2.5
BFS_S	42°3'16.38"N 19°10'10.63"E	42°2'49.14"N 19°11'35.11"E	Upper Triassic limestones and dolomites	ca. 2.3
KFS	42°3'14.84"N 19°14'4.52"E	42°2'39.09"N 19°18'36.87"E	Cretaceous and Middle - Upper Triassic limestones	ca. 7.4

Site	Location	Lithology
BFS_N	42°4'08.58"N / 19°09'50.72"E	see section BFS_N
BFS_S1	42°2'48.66"N / 19°11'13.86"E	see section BFS_S
BFS_S2	42°2'47.71"N / 19°11'18.70"E	see section BFS_S
KFS	42°2’52.22"N / 19°14'34.77"E	see section KFS

Table S4: Recent major earthquakes in the Italian Apennines for comparison with the Durrës (Albania) 2019, Montenegro 1979, Shkodra (Albania) 1905 and Dubrovnik (Croatia) 1667 earthquakes. Data compiled from Anicic et al. (1980), Kociaj and Sulstarova (1980), Decanini et al. (2000), Benetatos and Kiratzi (2006), Pondrelli et al. (2006), Chiarabba et al. (2009), MunichRE (2010, 2017), Albini and Rovida (2016), Chiaraluce et al. (2017), Markušić et al. (2017), Civico et al. (2018), The World Bank GPURL D-RAS Team (2019), Papadopoulos et al. (2020), Freddi et al. (2021) and the EMSC catalogue.

Date	Earthquake	Mw	Depth (km)	Casualties	Homeless	Economic loss	Aftershocks $M_w \geq 4$
24 Aug, 2016	Amatrice, I	6.0	4	↓	↓	↓	↓
26 Oct, 2016	Visso, I	5.9	8	300	20,000	26 bn $	45
30 Oct, 2016	Norcia, I	6.5	9	↑	↑	↑	↑
26 Apr, 2009	L'Aquila, I	6.3	9	300	60,000	2.5bn $	20
26 Sep, 1997	Umbria-Marche, I	6.0	10	10	?	3.5bn $	30
26 Nov, 2019	Durrës, AL	6.4	20-24	51	12 - 14.000	1 bn $	ca. 50
15 Apr, 1979	Bar, Montenegro	7.1	< 10	135	80,000	3.5bn $	90
01 Jun, 1905	Shkodra, AL	6.6	?	250	?	?	?
06 Apr, 1667	Dubrovnik, HR	7.1	12 (?)	2000-4000	13,000 (?)	"significant"	?

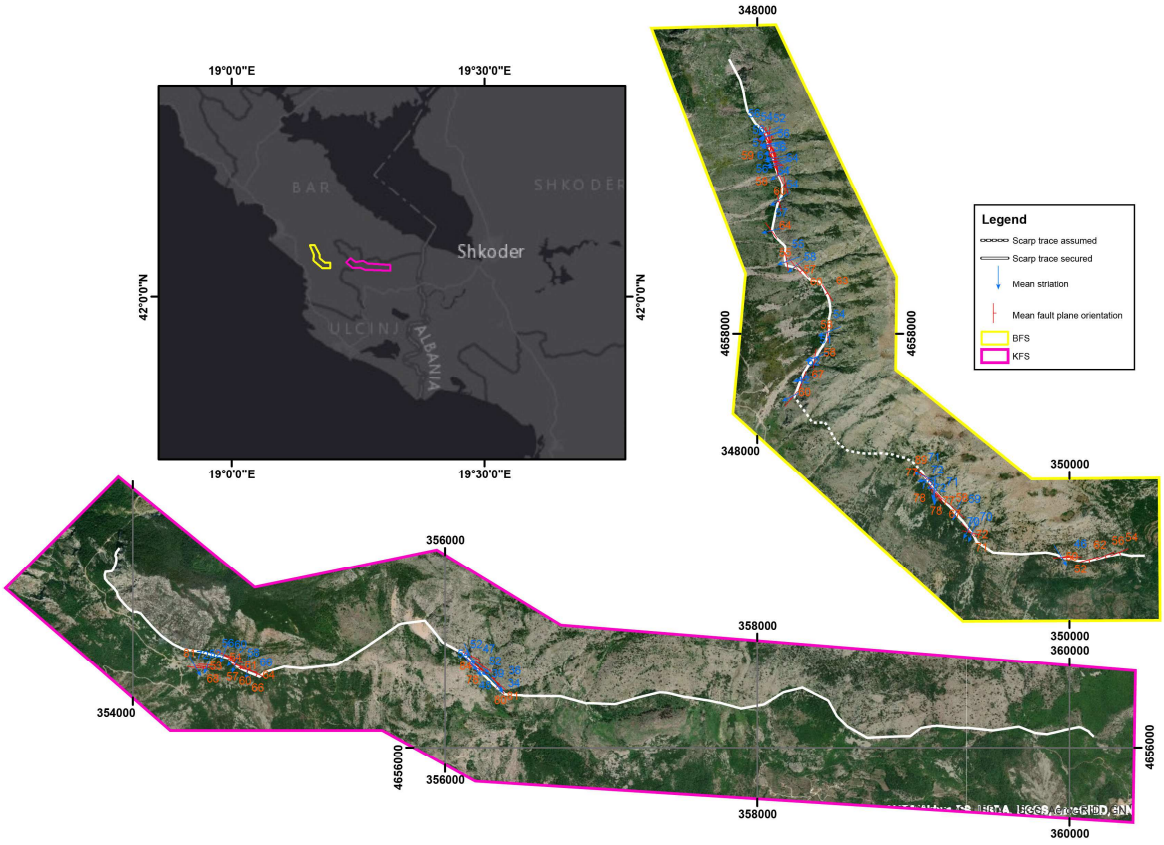

Figure S5: Satellite images with mean values of fault plane orientations and striations along the Bar Fault Scarp (BFS, yellow) and Katerkolle Fault Scarp (KFS, pink). Source of background (aerial) imagery: ESRI, DigitalGlobe, GeoEye, Earthstar Geographics, CNES Airbus DS, USDA, USGS, AeroGRID, IGN, HERE, Garmin, © Open Street Map contributors, and the GIS User Community.

Figure S6: Selection of earthquake ribbon field photographs. Single ribbons are indicated by dashed lines.

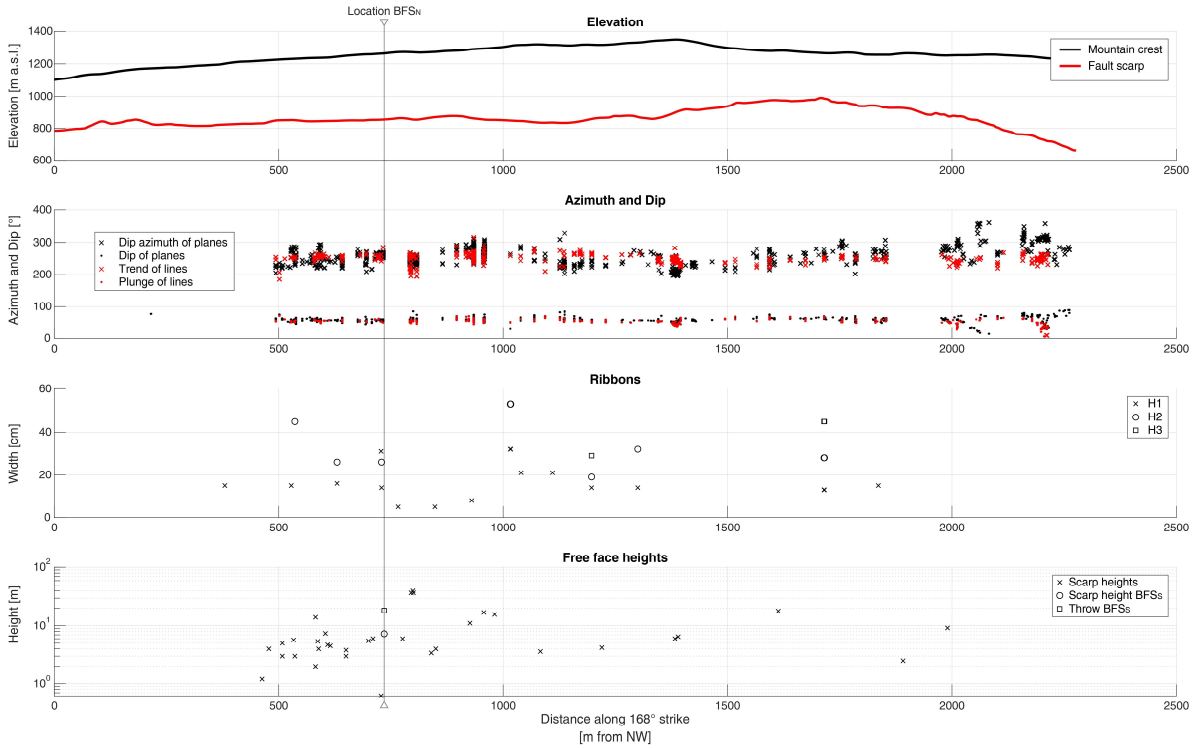

Figure S7 A: Fault scarp characteristics of BFS_N projected onto a line parallel to mean fault plane strike. We show (i) the elevation in m a.s.l. for the fault scarps and mountain crests above them, (ii) fault plane and striation orientations, (iii) the height of earthquake ribbons parallel to local striations and (iv) free face heights on logarithmic y-axis. The position of sampling location BFS_N, is indicated. For kilometrage see Figure S8.

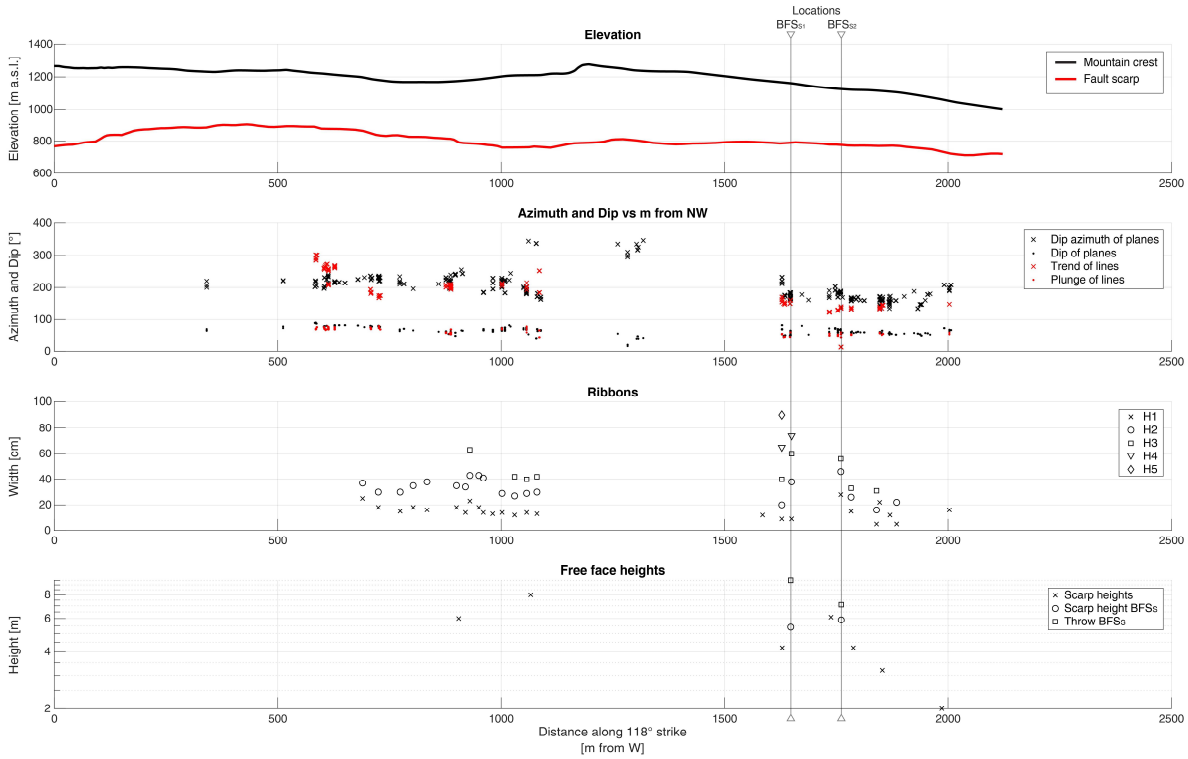

Figure S7 B: Fault scarp characteristics of BFS$_S$ projected onto a line parallel to mean fault plane strike. We show (i) the elevation in m a.s.l. for the fault scarps and mountain crests above them, (ii) fault plane and striation orientations, (iii) the height of earthquake ribbons parallel to local striations and (iv) free face heights on logarithmic y-axis. The positions of sampling locations BFS$_{S1}$ and BFS$_{S2}$ are indicated. For kilometrage see Figure S8.

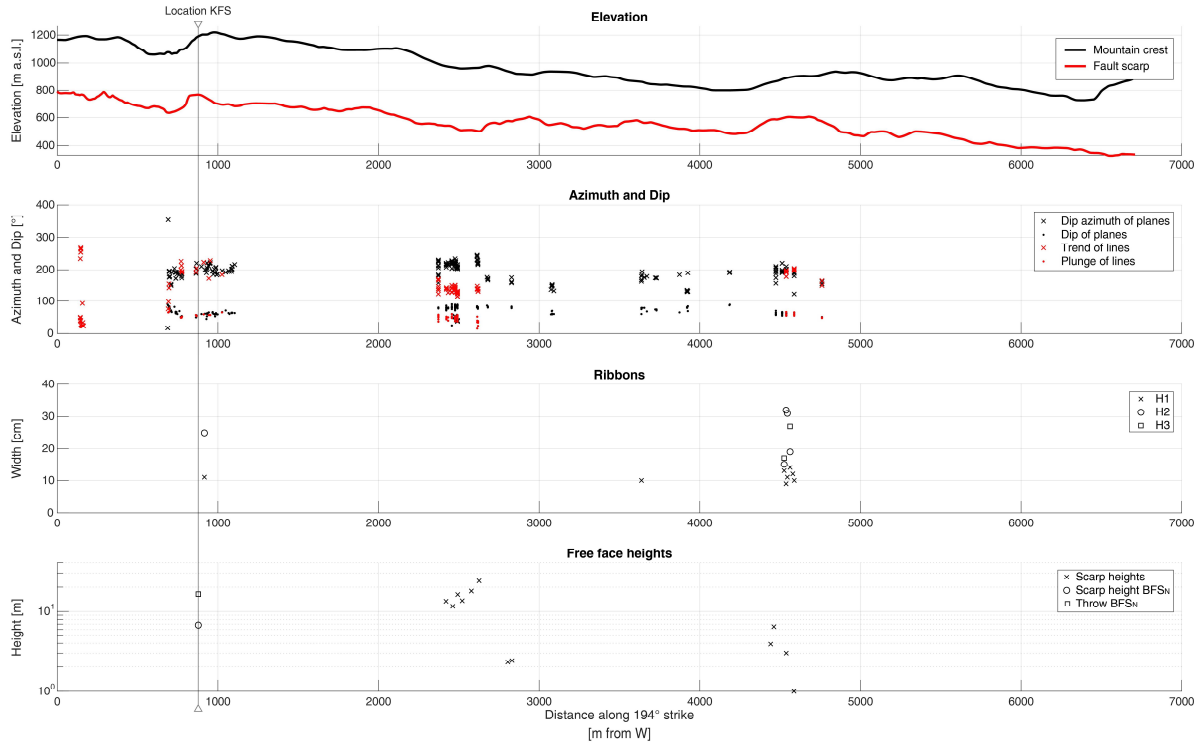

Figure S7 C: Fault scarp characteristics of KFS projected onto a line parallel to mean fault plane strike. We show (i) the elevation in m a.s.l. for the fault scarps and mountain crests above them, (ii) fault plane and striation orientations, (iii) the height of earthquake ribbons parallel to local striations and (iv) free face heights on logarithmic y-axis. The position of sampling location KFS is indicated. For kilometrage see Figure S8.

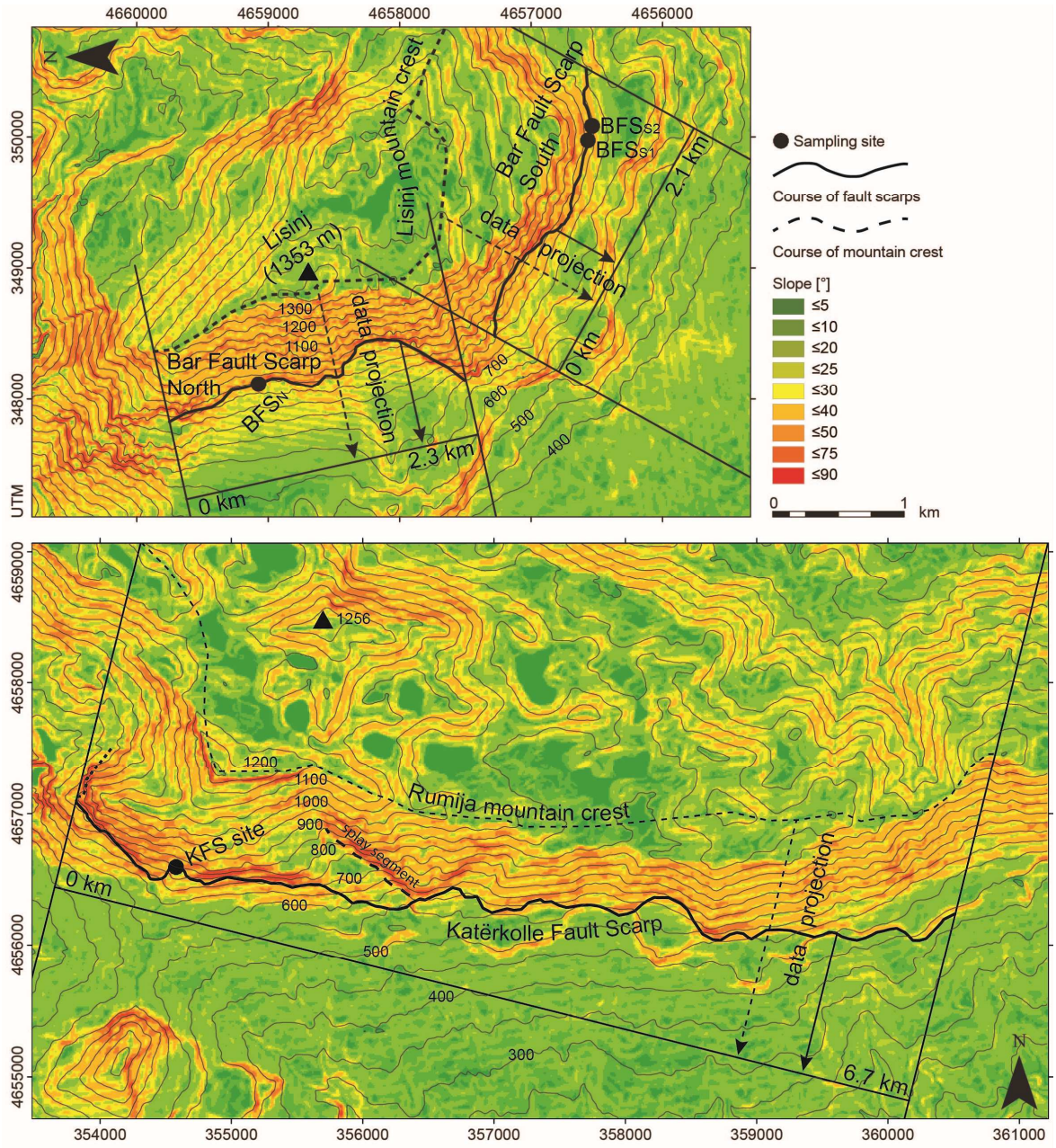

Figure S8: Maps showing TanDEM-X-based slope steepness around (a) BFS and (b) KFS and the geometry of data projection applied in Fig. S7. A significant slope steepness change with steep footwall slopes is observed downslope from the fault scarps.

Table S9: Moment magnitudes derived from empirical relationships after Wells & Coppersmith (1994). Values are based on two calculation principles, general faults (GF) vs. normal faults (NF), and different considered fault lengths (FL). It is stressed that owing to the setting described in the text, first-order structures possibly evoke magnitudes in a range ~1 M_w higher than the rates derived from fault scarp morphology. Minimum and maximum values are highlighted in bold. As simultaneous rupture of KFS and BFS_S is considered a likely scenario, the according value is bold and underlined. Calculation formula for FL (GF): $M_w = 5.08 + 1.16 * \log (FL)$; calculation formula for FL (NF): $M_w = 4.86 + 1.32 * \log (FL)$.

Rupturing Segment(s)	**BFS_{total}**	**BFS_N**	**BFS_S**	**KFS_{total}**	**BFS_S + KFS_{total}**	**BFS_{total} + KFS_{total}**	**BFS_{total}+ KFS_{total}+ connect.**
Length (km):	5.23	2.98	2.25	7.35	9.60	12.58	16.82
Magnitude (NF)	5.8 ± 1.6	5.5 ± 1.5	5.3 ± 1.4	6.0 ± 1.6	6.2 ± 1.6	6.3 ± 1.7	6.5 ± 1.7
Magnitude (GF)	5.9 ± 0.5	5.6 ± 0.4	**5.5** ± 0.4	6.1 ± 0.5	**<u>6.2</u>** ± 0.5	6.4 ± 0.5	**6.5** ± 0.5
Magnitude based on average (0.13 m) and max. (0.30 m) displacement (ribbons):							6.3 ± 0.1

Table S10: Long-term slip rates based on fault scarp profiles at sites BFS_N, BFS_S1, BFS_S2 and KFS (Fig. 5) and a proposed fault scarp formation age of 15 ± 3 kyr. The eventual rate presumes slip on the free face and its notional prolongation, the already eroded 'degraded scarp' (see also Fig. 5, e.g., Papanikolaou et al., 2005).

Sampling site	**Slope° F'wall**	**Slope° H' wall**	**Dip free face**	**Free face height**	**Full NFS height**	**Throw NFS**	**Long term rate [mm/yr]** *(based on full NFS height*
BFS_N	35°	33°	56°	8.8 m	22,2 m	18.4 m	**1.46± 0.37**
BFS_S1	35°	31°	55°	6.6 m	11,6 m	9.5 m	**0.77± 0.20**
BFS_S2	33°	28°	70°	6.2 m	7,6 m	7.1 m	**0.51± 0.12**
KFS	32°	27°	75°	7.0 m	17,0 m	16.4 m	**1.13± 0.28**

Tables S11, S12, S13: See xls file *'Tables_S11_S12_S13'*.

Table S14: ^{36}Cl dating: Modelling parameters.

Main production rates of ^{36}Cl in limestone at sea level and high latitude

- Spallation on Ca: 48.8 ± 3.4 atoms ^{36}Cl/g Ca/yr [*Stone et al.,* 1996]
- Spallation on K: 150 ± 18 atoms ^{36}Cl/g K/yr [*Marrero et al.,* 2016]
- Spallation on Ti: 13 ± 3 atoms ^{36}Cl/g Ti/yr [*Fink et al.,* 2000]
- Spallation on Fe: 1.9 ± 0.2 atoms ^{36}Cl/g Ti/yr [*Stone,* 2005]
- Slow negative muon stopping rate at land surface:
- 190 muons/g/yr [*Heisinger et al.,* 2002]
- Neutron attenuation length: 208 g/cm^2 [e.g., *Gosse and Phillips,* 2001]
- Neutron apparent attenuation length for a horizontal unshielded surface: 160 g/cm^2 [*Gosse and Phillips,* 2001]
- Negative muon apparent attenuation length for a horizontal unshielded surface: 1500 g/cm^2 [*Heisinger et al.,* 2002]
-

Parameters for the sampling site at the site Bar north of the Bar fault (BFS_N)

- Latitude = 42.0691°N; Longitude = 19.1641°E
- Elevation = 831 m a.s.l.
- For a constant geomagnetic field [*Stone,* 2000]: $S_{el,f}$ = 1.968 and $S_{el,\mu}$ = 1.407
- Chemical composition of rock and colluvium: see table S2
- Hanging wall dip α = 33°
- Fault plane dip β = 56°
- Footwall dip γ = 35°
- Height up the fault scarp H = 22.2 m (height up the free-face = 8.45 m)
- Mean rock density ρ_{rock} = 2.55 g/cm^3 (from sample weight and water suppression amount)
- Mean colluvial density ρ_{coll} = 1.5 g/cm^3
- Erosion rate of the free-face = 0.001 mm/yr
- Pre-exposure = 1 kyr (apparent exposure time of the hillslope before the fault scarp developed)*
- Topographic shielding = 0.940 (top of the free-face)
- Snow cover influence is assumed as negligible
- Vegetational influence is assumed as negligible

*A pre-exposure of 1 kyr results in a reasonable modelling pattern and is similar to other published studies (e.g., Mechernich et al., 2018). We tested other values and the resulting slip rates and EQ ages agree within +-20%.)

References

Albini, P. and Rovida, A.: From written records to seismic parameters: the case of the 6 April 1667 Dalmatia earthquake, Geosci. Lett., 3 (30), doi: 10.1186/s40562-016-0063-2, 2016.

Anicic, D., Berz, G., Boore, D., Bouwkamp, J., Hakenbeck, U., McGuire, R., Sims, J., Wieczorek, G., Matthiesen, R.B., in Leeds, A. (Ed.): Reconnaissance Report Montenegro, Yugoslavia Earthquake April 15, Earthquake Engineering Research Institute, Oakland, CA, USA, 1980.

Benetatos, C. and Kiratzi, A.: Finite-fault slip models for the 15 April 1979 (Mw 7.1) Montenegro earthquake and its strongest aftershock of 24 May 1979 (Mw 6.2), Tectonophysics, 421, 129-143, 2006.

Chiarabba, C. et al.: The 2009 L'Aquila (central Italy) M_w6.3 earthquake: Main shock and aftershocks, Geophys. Res. Let., 36, 2009.

Chiaraluce, L. et al.: The 2016 Central Italy Seismic Sequence: A First Look at the Mainshocks, Aftershocks, and Source Models, Seismol. Res. Lett., 88 (3), 757-771, 2017.

Civico, R., Pucci, S., Villani, F., Pizzimenti, L., De Martine, P.M., Nappi, R. and the Open EMERGEO Working group: Surface ruptures following the 30 October 2016 M_w 6.5 Norcia earthquake, central Italy, J. Maps, 14(2), 151-160, 2018.

Decanini, L., Gavarini, C. and Mollaioli, F.: Some remarks on the Umbria-Marche earthquakes of 1997, European Earthquake Engineering, 14(3), 18-48, 2000.

Fink, D., Vogt, S. and Hotchkis, M.: Cross-sections for ^{36}Cl from Ti at E_p = 35-150 MeV: Applications to in-situ exposure dating, Nucl. Instrum. Methods Phys. Res, 172, 861-866, 2000.

Gosse, J. C., and Phillips, F.M.: Terrestrial in situ cosmogenic nuclides: theory and application, Quat. Sci. Rev., 20, 1475-1560, 2001.

Freddi, F., Novelli, V., Gentile, R., Veliu, E., Andreev, S., Andonov, A., Greco, F. and Zhuleku, E.: Observations from the 26th November 2019 Albania earthquake: the earthquake engineering field investigation team (EEFIT) mission, Bull. Earthq. Eng. 19(5), 2013-2044, 2021.

Heisinger, B., Lal, D., Jull, A.J.T., Kubik, P., Ivy-Ochs, S., Knie, K. and Nolte, E.: Production of selected cosmogenic radionuclides by muons: 2. Capture of negative muons, Earth Planet. Sci. Lett., 200, 357-369, 2002.

Kociaj, S. and Sulstarova, E.: The earthquake of June 1, 1905, Shkodra, Albania; Intensity distribution and macroseismic epicentre, Tectonophysics, 67 (3-4), 319-332, 1980.

Markušić, S., Ivančić, I., and Sović, I.: The 1667 Dubrovnik earthquake–some new insights, Studia Geophys. et Geod. 61 (3), 587-600, 2017.

Marrero, S. M., Phillips, F. M., Caffee, M. W. and Gosse, J. C.: CRONUS-Earth cosmogenic ^{36}Cl calibration, Quat. Geochronol., 31, 199–219, 2016.

MunichRE: Topics Geo, Naturkatastrophen 2009, Analysen, Bewertungen, Positionen, Munich, Germany, 2010.

MunichRE: Topics Geo, Natural catastrophes 2016, Analyses, assessments, positions. Munich, Germany, 2017

Papadopoulos, G. A., Agalos, A., Carydis, P., Lekkas, E., Mavroulis, S., and Triantafyllou, I.: The 26 November 2019 Mw 6.4 Albania Destructive Earthquake, Seismol. Res. Lett., 91, 3129-3138, 2020.

Papanikolaou, I.D., Roberts, G.P. and Michetti, A.M.: Fault scarps and deformation rates in Lazio-Abruzzo, Central Italy: Comparison between geological fault slip-rate and GPS data, Tectonophysics, 408, 147-176, 2005.

Pondrelli, S., Salimbeni, S., Ekström, G., Morelli, A., Gasperini, P. and Vannucci, G.: The Italian CMT dataset from 1977 to the present, Phys. Earth Planet. Inter., 159, 286-303, 2006.

Schlagenhauf, A., Y. Gaudemer, L. Benedetti, I. Manighetti, L. Palumbo, I. Schimmelpfennig, R. Finkel, and K. Pou: Using in situ Chlorine-36 cosmonuclide to recover past earthquake histories on limestone normal fault scarps: a reappraisal of methodology and interpretations, Geophys. J. Int., 182, 36 - 72, doi:10.1111/j.1365-246X.2010.04622, 2010.

Stone, J. O., Allan, G. L., Fifeld, L.K. and Cresswell, R. G.: Cosmogenic chlorine-36 from calcium spallation: Geoch. Cosmochim. Acta, 60 (4), 679-692, 1996.

Stone, J. O.: Air pressure and cosmogenic isotope production, J. Geophys. Res., 105, 23753-23759, 2000.

Stone, J. O.: Terrestrial chlorine-36 production from spallation of iron, 10th AMS Conference, Berkeley, USA, 2005.

The World Bank GPURL D-RAS Team: M6.4 Albania Earthquake Global Rapid Post Disaster Damage Estimation (GRADE) Report, 2019.

Wells, D.L. and Coppersmith, K.J.: New empirical relationships among magnitude, rupture length, rupture width, rupture area, and surface displacement, B. Seismol. Soc. Am., 84, 4, 974-1002, 1994.